Macromolecules

ARTICLE

pubs.acs.org/Macromolecules

Rheo-Optical Study on Dynamics of Bottlebrush-Like Polymacromonomer Consisting of Polystyrene.

Hiroshi Iwawaki,[†] Tadashi Inoue,*[,†] and Yo Nakamura[‡]

[†]Department of Macromolecular Science, Graduate School of Science, Osaka University, 1-1 Machikaneyama-cho, Toyonaka, Osaka 560-0043, Japan

[‡]Department of Polymer Chemistry, Graduate School of Engineering, Kyoto University, Katsura, Nishikyo-ku, Kyoto 615-8510, Japan

ABSTRACT: Dynamic birefringence and viscoelastic measurements of bottlebrush-like polystyrene polymacromonomer were conducted over a wide frequency region covering from the glass-to-rubber transition zone to the flow zone in order to discuss effects of highly branched structure on polymer chain dynamics. Strain-induced birefringence at high frequencies was negative, similarly to linear polystyrenes, while it was positive in the flow zone, indicating the main chain segment has positive optical anisotropy. By using the modified stress-optical rule (MSOR), the complex modulus was decomposed into two components, main chain and branch components. The dynamical stiffness of main chain (number of repeating units per viscoelastic segment) was found to be approximately 10 times larger than that for linear polystyrenes. The cooperative motion of the side chains originated by the repulsive interaction between the branches was strongly suggested.

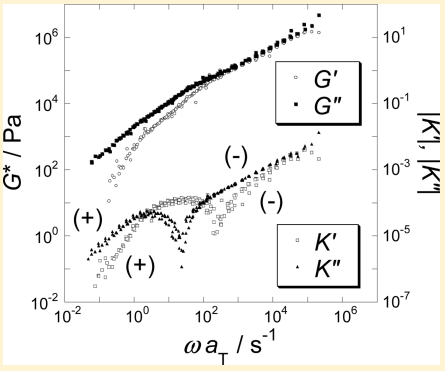

INTRODUCTION

Viscoelastic properties and molecular dynamics of polymer melts have long been studied experimentally and theoretically.[1−3] One of the most important molecular concept to understand the viscoelastic properties is the "viscoelastic segment", which is defined as the smallest subchain for molecular expression of stress. For the case of polystyrene (PS), the molecular weight of the viscoelastic segment in melt is estimated as 850 by the rheo-optical method.[4] This value is close to the Kuhn statistical segment size.[5] Thus, the definition of the viscoelastic segment seems to be reasonable and clear for linear chains. However, this is not true for polymer chains having complex chain architectures. For example, if many long branches are densely connected to the repeating units of the main chain, the segment size of main chain would become larger than that for linear chains because of repulsive interaction between the branches.

Polymerization of macromonomers is one of the methods to produce highly branched polymers in addition to grafting the side chain onto a prepared linear chain.[6] Controlling the molecular weight of macromonomer and polymerization condition of macromonomer, the ratio of the polymerization index of branch, n_B, to main chain, n_M, $R = n_B/n_M$, can be varied. For the case of $R \ll 1$, polymacromonomers, PMs can be regarded as "molecular brushes" while $R \gg 1$, PMs can be regarded as "hyperbranched (star) polymers". PMs having molecular brush shape behave as semiflexible chains in solution.[7−9] Terao et al. studied chain dimension of PMs consisting only of polystyrene units in solution.[10−13] They showed that the contour length per main-chain residue is insensitive to the branch length, while the Kuhn segment length λ^{-1} under the Θ condition remarkably increases with increasing the branch length. They concluded that in addition to the high segment density around the main chain, "repulsions" between the main chain and side chain and between neighboring side chains play an important role in the high stiffness of polymacromonomers.[14]

In this study, we investigate the viscoelastic properties of PMs as a model polymer to scrutinize the effects of highly branched structure on polymer dynamics. We will show that the highly branched structure provides different dynamics from those of linear polymers or scarcely branched polymers. For the case of bottlebrush type PMs, the complex shear modulus G^* reflects two different chain dynamics corresponding to the branches and the main chain.[15,16] However, it would be difficult to separate the dynamics of each component from only viscoelastic measurements and therefore details of the dynamics of them have not been discussed.

The rheo-optical method using birefringence measurements is a useful technique to study the size and reorientation process of the viscoelastic segment.[4] When rubbery materials are deformed, the birefringence as well as the stress is observed. The origin of both the strain-induced birefringence and the stress is the orientation of the segments. A proportional relation called the stress-optical rule (SOR) holds well between the deviatoric parts of the stress tensor and the refractive index tensor.[17] For the case of oscillatory shear deformations, SOR may be written as follows.

$$K^*(\omega) = CG^*(\omega) \quad (1)$$

Here, $G^*(\omega)$ is the complex shear modulus and $K^*(\omega)$ is the complex shear strain-optical coefficient defined as the complex

Received: April 11, 2011
Revised: May 25, 2011
Published: June 13, 2011

Table 1. Characterization of Samples and Optical Parameters

sample code	$M_B/10^3$	$M_{total}/10^6$	n_B	n_M	$C_B/10^{-9}$ Pa^{-1}	$C_M/10^{-9}$ Pa^{-1}
PM65	6.77	1.32	65.1	195	−2.79	34.6
PM15[a]	1.65	1.23	15.9	745	−2.7	−9.5

[a] Examined in the previous study.

ratio of the birefringence to the strain. The proportional coefficient, C, called the stress-optical coefficient, can be related with the anisotropy of polarizability of the segment.[18,19] Therefore, C is a measure of the segment size.

In a previous study, Inoue et al. reported the rheo-optical data on a PM in a range of frequencies covering from the glassy zone to the rubbery zone and they showed that branched chain and main chain components have different stress-optical coefficients.[20] The different stress-optical coefficients make it possible to separate the shear modulus into branch and main chain components. Concerning the main chain component, they concluded that the viscoelastic segment size was larger than that for ordinary linear PS. However, their data do not fully cover the terminal flow region because they used tensile type rheometer. In addition, they reported the data for only one PM, and questions such as effects of branch length have not been discussed. In this paper, we provide the results of the simultaneous measurement of the dynamic birefringence and the dynamic viscoelasticity for a different PM in a wide range of frequencies covering from the glass transition zone to the terminal flow zone by using a new rheo-optical apparatus based on oblique laser beam method.[21] We will show the birefringence originated by orientation of the branch is negative while the birefringence by main chain segment is positive. The obtained data are analyzed with the modified stress-optical rule (MSOR). The modulus, G^*, of PMs was decomposed into two components, corresponding to the main chain and the branch motions. We will discuss the dynamical stiffness of main chain and cooperative motion of branches originated by the repulsive interaction between the branches.

EXPERIMENTAL SECTION

Sample. Polystyrene polymacromonomer, (sample code PM65), which has the PS structure in both the main chain and the branches, was synthesized in the manner reported by Tsukahara et al.[22] Styrene was anionically polymerized in toluene using tolyllithium as an initiator, and the reaction was terminated by *p*-chloromethylstyrene (Seimi Chemical Co. Ltd.) to obtain the macromonomer. The product was reprecipitated several times into methanol to remove unreacted *p*-chrolomethylstyrene. Its weight-average molecular weight M_w was 6770 determined by light scattering, and the number of sample code indicates the degree of polymerization of the macromonomer. The macromonomer thus purified was polymerized in benzene at 40−60 °C with azobisisobutylonitrile as an initiator to obtain the polymacromonomer sample. The weight-average molecular weight M_w and M_w/M_n were 1.32×10^6 and 1.14 respectively.[13,23] Characteristics of the sample are summarized in Table 1.

For rheo-optical measurements, pellets were prepared by being melted in a vacuum oven at 180 °C and then cooled down to the room temperature.

Rheo-Optical Measurements. The apparatus for rheo-optical measurement on oscillatory shear deformation was reported elsewhere.[24] A structure of the rheometric and optical parts of the device is sketched

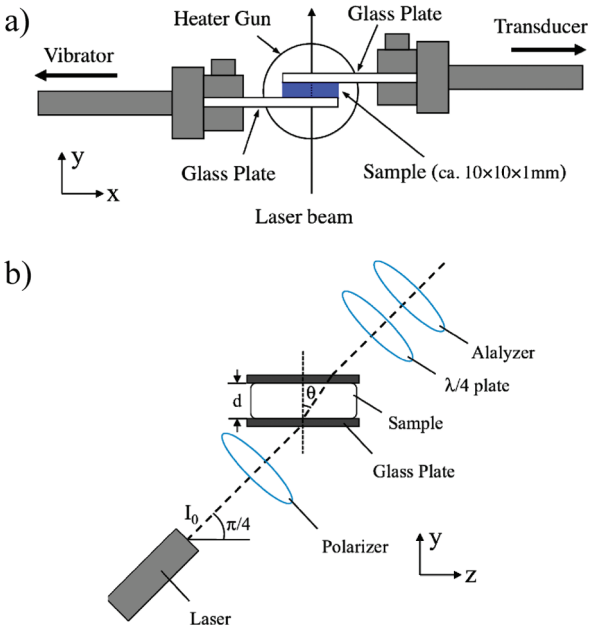

Figure 1. Schematic illustration of the viscometric parts (a) and the optical parts of the parallel-plate fixture for birefringence measurements (b).

in Figure 1, parts a and b, respectively. As in the viscoelastic measurements, a small amplitude oscillatory deformation, $\gamma(t) = \gamma_0 \sin \omega t$ (with $\gamma_0 = 0.06$) is applied on the sample sandwiched between two glass plates.

Then, the birefringence of the sample is obtained as a sinusoidal function of t:

$$\Delta n^Z(t) = 2\gamma_0 K_0(\omega) \sin[\omega t + \delta_B(\omega)]$$
$$= 2\gamma_0 K'(\omega) \sin \omega t + 2\gamma_0 K''(\omega) \cos \omega t \quad (2)$$

The phase angle $\delta_B(\omega)$ appearing in eq 2 may be different from the viscoelastic phase angle, $\delta(\omega)$. The coefficient of 2 is needed to convert directly measured Δn^Z ($=\Delta n_{xx} - \Delta n_{yy}$) to Δn_{xy} under small strain. (Δn_{ij} represents the ij component of deviatoric part of the refractive index tensor) A complex strain-optical coefficient can be defined as $K^* = K' + iK''$ with $K'(\omega) = K_0(\omega) \cos \delta_B(\omega)$ and $K''(\omega) = K_0(\omega) \sin \delta_B(\omega)$, as similar to the expression of the complex modulus.

In the measurement of $\Delta n^Z(t)$, the incident light of intensity I_0 is applied and the intensity of the light transmitted the system $I_\omega(t)$, for a given ω, is recorded against t on displacing the analyzer from the crossed nicol by a small angle α. (The light path of the measurements is shown in thick dashed lines in Figure 1b.) Then, $\Delta n^Z(t)$ is proportional to a ratio between I_ω and I_0 as:[21,24]

$$\Delta n^Z(t) = \frac{\lambda_{wl}}{2\pi d\alpha} \frac{\Delta I_\omega(t)}{T_0} \frac{1}{\tan \theta} \quad (3)$$

Here, λ_{wl} is the wavelength in vacuum, d is the thickness of the sample, and θ is the refraction angle, as indicated in Figure 1b.

The shear modulus, $G^*(\omega)$, and $K^*(\omega)$ were determined in the temperature ranging from 120 to 190 °C. To check the consistency of the data, $G^*(\omega)$ was measured with a Rheometric ARES system with a homemade parallel plate fixture having 4 mm diameter.

Instrument compliance is known to be an important issue in the rheological measurements in the glassy zone. Following the method reported McKenna et al., the compliance of the apparatus was corrected.[25,26] In their method, the apparatus is assumed to be connected in series with

dx.doi.org/10.1021/ma2008332 |*Macromolecules* 2011, 44, 5414–5419

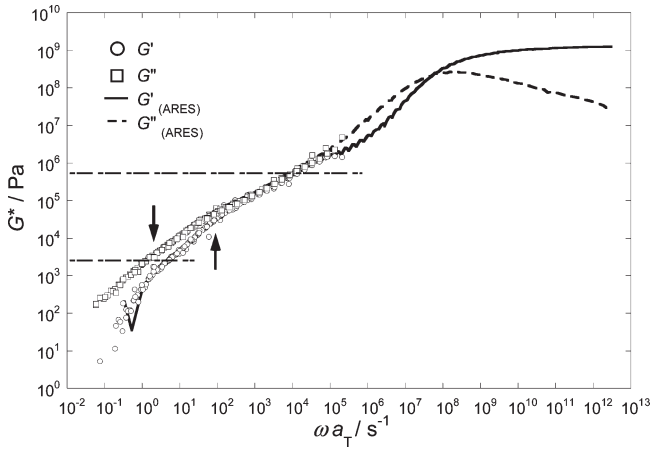

Figure 2. Composite curves of the complex shear modulus G^* for PM65 measured with shear flow birefringence apparatus. Lines represent the G^* data determined by ARES. The reference temperature is 140 °C.

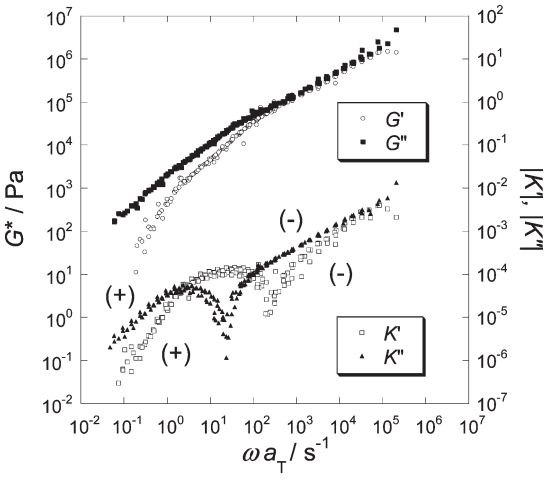

Figure 3. Composite curves of G^* and the complex strain-optical coefficient in shear deformation K^* for PM65. The reference temperature is 140 °C.

the viscoelastic sample. Thus, the measured compliance is a sum of the compliances of the sample and the apparatus.

$$J_{mes}^* = J_s^* + J_a^* \tag{4}$$

Here J_{mes}^* is the measured compliance, J_s^* is the actual complex sample compliance, and J_a^* is the apparatus compliance. The apparatus compliance can be estimated by using hard samples such as steel plates. The true sample modulus, $G^* = 1/J_s^*$, could be obtained with eq 5.

$$G^* = \frac{1}{J_s^*} = \frac{1}{J_{mes}^* - J_a'} \tag{5}$$

This correction was also made for the rheo-optical apparatus. By correcting the apparatus compliance, true G^* and K^* could be obtained.[27]

RESULTS AND DISCUSSION

Composite Curves for $G^*(\omega)$ and $K^*(\omega)$. Figure 2 shows the composite curves for G^* from the transition region to the flow region. Here we used the method of reduced variables.[28] Also included is G^* data determined by ARES. In the frequency range ($\omega a_T < 1 \times 10^3$ s^{-1}), the obtained G^* data are in accord with ARES data.

As shown in Figure 2, G' and G'' show a power law relationship, $G' \sim G'' \propto \omega^{1/2}$, at high frequencies ($\omega a_T > 1 \times 10^2$ s^{-1}). Similar frequency dependence was observed for polymacromonomers having different chemical structures in main and side chains[29] and also for cross-linked molecular brushes.[30] At lower frequencies than down-arrow ($\omega a_T = 1 \times 10^0$ s^{-1}), G' and G'' show the terminal relaxation behavior, $G' \propto \omega^2$ and $G'' \propto \omega^1$. At middle frequencies a weak shoulder appears in G' as indicated by up-arrow ($\omega a_T = 1 \times 10^2$ s^{-1}). These two relaxations of G' are also observed for the comb-like polymers.[31] The two-step relaxation of G' strongly suggests that G^* is composed of two components, corresponding to the fast motion of the branch in higher frequency region and the slow motion of the main chain in lower frequency region.

Since the molecular weight of branches ($M_B = 6670$) is much lower than the molecular weight of entanglement strand ($M_e \sim 18000$) there is no entanglements between branches. On the other hand, the molecular weight of trunk ($M_T = 2.0 \times 10^4$) is comparable to M_e. Considering that the effective concentration of trunks is quite low ($\sim 1/n_B$), we conclude that there is no entanglements between any chains. The dynamics of bottle-brush like polymacromonomers may be similar to combs having short branches. The hierarchical relaxation of the comb architecture implies that there will be distinct relaxation modes at intermediate and low frequencies corresponding to the branches and backbone, respectively. In general, the intermediate frequency plateau is a consequence of the branch relaxation, during which the backbone is essentially frozen due to the presence of the branch points. As suggested by Kirkwood et al., the short length of the branches will allow us to make analogueies to the behavior of short multiarm stars.[32] Thus, in the flowing discussion, we compare the PM to star chains. According to the Rouse theory or the Rouse−Ham theory for star arms,[33,34] the height of modulus of the slowest mode of linear chains or the branch of star polymers is related to the molecular weight. Lower dashed-dotted line in Figure 2 represents

$$G' = \frac{\rho RT}{M_{total}} \tag{6}$$

Here, ρ, R, and T are the density, gas constant, and temperature, respectively. M_{total} represents the whole molecular weight of the PM. This estimation agrees with the height of modulus in the terminal flow region around $\omega \sim 1$ s^{-1}. This means that relaxation in the terminal flow region is governed by the molecular motion of whole molecules. On the other hand, upper dashed-dotted line in Figure 2 represents

$$G' = \frac{\rho RT}{M_B} \tag{7}$$

Here, M_B represents the molecular weight of a single branch of PM. This estimation is more than ten times larger than the experimental value for the low frequency end of the branch relaxation around $\omega \sim 100$ s^{-1}. This result clearly shows that the relaxation does not reflect the motion of the single branch and strongly suggest the cooperative motion of more than 10 branches.

Figure 3 shows the composite curves of G^* and K^* from the transition region to the flow region. The sign of K^* is negative in high frequency region and positive in low frequency region although all repeating units for both of main chain and branch are styrene. Since relaxation of main chain segment is anticipated

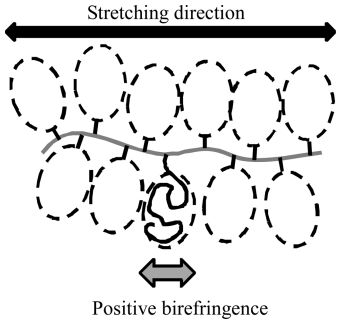

Figure 4. Schematic illustration of polymacromonomer.

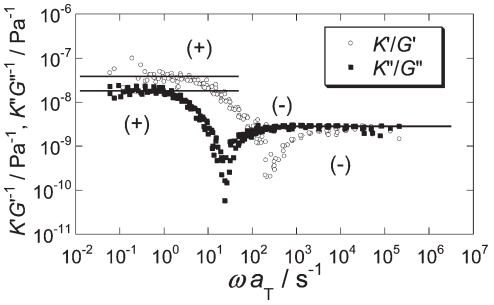

Figure 5. Frequency dependence of the ratio of K'/G' and K''/G'' for PM65. The reference temperature is 140 °C.

to be observed at low frequencies, it would be a reasonable assignment that the branch shows negative birefringence and the main chain shows positive birefringence. The positive birefringence of the main chain could not be observed for PM having shorter branches.[20]

The Origin of Positive Birefringence of Main Chain and the Shape of Relaxed Branches. As described above, the positive birefringence was observed in the flow region. However, for the case of linear PS in melt, the birefringence originated by the segment orientation is always negative because the anisotropy of polarizability of repeating units is negative.[4] Since each repeating unit of the PM has the long branches, the branches may optically contribute to the main chain component. If there is no interaction between neighboring branches, they would take the sphere-shaped random coil conformation and the branches would not show any optical anisotropy. In this context, the branches do not contribute to the birefringence originated by the orientation of main chain segment. However, PMs have highly branched structure, the branches would be extended or stretched in perpendicular direction to main chain axis and would have an oval sphere shape (see Figure 4), in a similar way in dilute solutions[10] or the dense polymer brushes on a flat surface.[35] This shape has some large polarizability anisotropy along the main chain, and therefore the main chain component shows positive birefringence.

Modified Stress-Optical Rule (MSOR). For the case of PMs, SOR does not hold well between the strain-induced birefringence and the stress in the rubbery zone. This is because both the stress and the birefringence include two relaxation modes corresponding to the motions of the main and the branch components. For such a case, G^* and K^* are the sums of the two components and can be written as follows.[20]

$$G^* = G_M^* + G_B^* \tag{8}$$

$$K^* = K_M^* + K_B^* \tag{9}$$

Here, the subscripts represent the main and the branch components. MSOR assumes that SOR holds well for each component. Equation 9 can be rewritten as follows.

$$K^* = C_M G_M^* + C_B G_B^* \tag{10}$$

It is expected that SOR holds valid for each component because the birefringence and the stress of both two components are originated in orientation of the main chain segment and the branch segment, respectively. According to the different signs of the birefringence between the main chain component and the branch component, the segments of the two components can be also different in structure. Thus, the two components may have the different stress-optical coefficients, C_M and C_B. The coefficients could be determined experimentally from the ratio of K' to G', K'/G'. Note that the proportional coefficient in SOR, C, is independent of frequencies. Figure 5 shows frequency dependence of K'/G' and K''/G''. In this figure, both K'/G' and K''/G'' show two limiting values at high frequencies and low frequencies. The limiting value of K'/G' and K''/G'' at high frequencies would correspond to C_B because the branch component would be dominant in this region.

According to MSOR, the ratio can be estimated as follows.

$$\frac{K'}{G'} = \frac{K_M' + K_B'}{G_M' + G_B'} = \frac{C_M G_M' + C_B G_B'}{G_M' + G_B'} \tag{11}$$

If $G_M' \ll G_B'$ and $C_M \sim C_B$ at high frequencies, then eq 11 can be written approximately

$$\frac{K'}{G'} \sim \frac{C_B G_B'}{G_B'} = C_B \tag{12}$$

Thus, the limiting value of K'/G' and K''/G'' at high frequencies, -2.79×10^{-9} Pa^{-1}, corresponds to C_B.

On the other hand, at lower frequencies than the inverse of relaxation time, the asymptotic relationships, $G' = A_G\omega^2$ and $G'' = \eta\omega$, hold valid, and therefore eq 11 may be written as follows.

$$\frac{K'}{G'} = \frac{C_M A_{G,M}\omega^2 + C_B A_{G,B}\omega^2}{A_{G,M}\omega^2 + A_{G,B}\omega^2} = \frac{C_M A_{G,M} + C_B A_{G,B}}{A_{G,M} + A_{G,B}} \tag{13}$$

$$\frac{K''}{G''} = \frac{C_M \eta_M \omega + C_B \eta_B \omega}{\eta_M \omega + \eta_B \omega} = \frac{C_M \eta_M + C_B \eta_B}{\eta_M + \eta_B} \tag{14}$$

Thus, K'/G' and K''/G'' give a different average of C_M and C_B. Naturally, $A_{G,M} \gg A_{G,B}$ and therefore K'/G' would be very close to C_M. Thus, from the limiting value of K'/G', C_M was estimated 3.46×10^{-8} Pa^{-1}.

Solving the simultaneous equation of eqs 8 and 10 for G_M^* and G_B^* at each temperature, the complex modulus G^* could be decomposed into two components. The obtained composite curves for G_M^* and G_B^* are shown in Figure 6. Here the method of reduced variable was used separately. At the low frequencies ($\omega a_T \approx 2 \times 10^0$ s^{-1}), the full relaxation behavior of the main chain component is observed for the first time in this study.

G_B' and G_B'' are similar to the Rouse model representing the dynamics for the linear polymers without entanglements, suggesting that the entanglement between branches can be ignored. However, we should note that C_B of the PM is about half of the stress-optical coefficient for linear PS ($C_R = -4.8 \times 10^{-9}$ Pa^{-1}).[4]

dx.doi.org/10.1021/ma2008332 |*Macromolecules* 2011, 44, 5414–5419

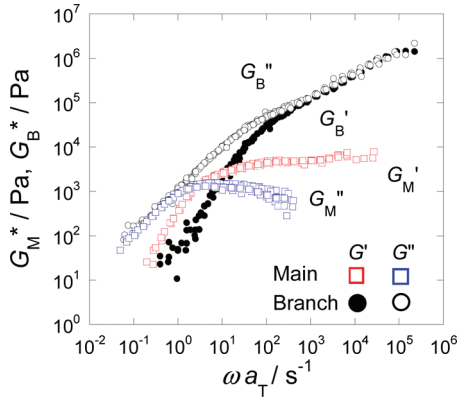

Figure 6. Decomposition of G^* into two components G_M^* and G_B^* for PM65. The reference temperature is 140 °C.

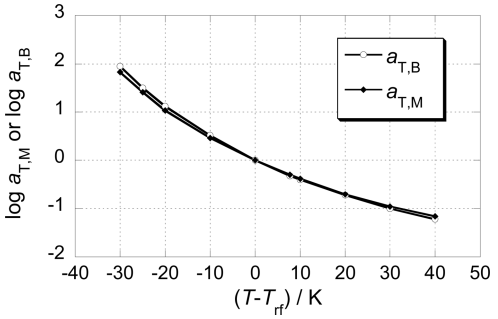

Figure 7. Temperature dependence of the shift factors for G_M^* and G_B^*. The reference temperature is 140 °C.

This result suggests that the branch segment causes the stress about twice larger than the linear chains under the same deformation. This is probably due to an elastic coupling originated by the repulsive interaction between the neighboring branches. Therefore, in order to describe G_B^*, the conventional bead−spring theory should be modified by taking into account the coupling between the branches. A comment may be needed for the Rouse-like behavior of the branches. One may wonder whether this Rouse-like behavior is compatible with the cooperative motion of branches, which may be much different from linear nonentangled polymer motions. We note that the Rouse-like behavior does not depend on details of molecular model. It would be observed commonly for coupled oscillations. For example, the damped torsional oscillator model provides the same frequency dependence. We believe that the elastic coupling between the branches would be described with some sort of coupled oscillations, which results in the Rouse-like behavior.

A further comment may be needed for the limitation of the simply additive laws of eqs 8 and 10. As described before, the origin of positive birefringence of main chain can be attributed to oval shape (stretched chain conformation) for the branch, which strongly depends on the density of branch points. In this context, it is obvious that C_M depends on the branch chain length and the density of branch points. For example, if the density of branch points decreases, the conformation of branch approaches a Gaussian, and the branch would not show any effective optical anisotropy. In such a case, C_M and C_B would agree with each other like scarcely branched chains, and the two equations of 8 and 10 becomes equivalence.

The limiting modulus of G_M' at high frequencies may be related to the viscoelastic segment size (molecular weight) of main chain, M_S^{main}.

$$M_S^{main} = \frac{\rho RT}{G_M'} \tag{15}$$

The estimated value of M_S^{main} was 7.39×10^5. The number of repeating unit per main chain segment, M_S^{main}/M_B, was calculated as 109. This value is slightly smaller than the corresponding value (133) for the Kuhn segment size in cyclohexane solutions.[13] This difference remains to be investigated. Detailed study using different M_B is in the planning stage.

Figure 7 shows temperature dependence of two shift factors, $a_{T,M}$ and $a_{T,B}$ used for constructing the composite curves for G_M^* and G_B^* shown in Figure 6. Since G_B^* reflects the elastic coupling of braches due to the repulsive interaction, which may depend on temperature, the two shift factors could be different. However, a quite similar temperature dependence of $a_{T,M}$ and $a_{T,B}$ was observed as far as we studied. The present result suggests that the main chain and the branch component have the almost same activation energy in their reorientation process. In other words, our PM can be regarded as thermorheologically simple in first approximation. We note that the present result is in accord with the pioneer study by Tsukahara et al.[15] and other rheological studies on polymacromonomers.[29,30]

CONCLUSION

By using the shear apparatus, for the first time ever, we conducted the measurement of the dynamic birefringence on bottlebrush like polymacromonomer in the full wide range of frequencies covering from the rubbery transition region to the terminal flow region. The sign of birefringence corresponding to the main chain component was first reported to be positive, contrasting to that the sign of the ordinary linear PS is negative in these regions. The positive birefringence indicates that the shape of the relaxed branch is oval sphere having a long axis at right angles to the main chain backbone.

With using modified stress-optical rule (MSOR), G^* of PMs was decomposed into two components, the main chain and the branch motions. G^* of branch component cannot be described with dynamics of single branch. We speculated that there is the elastic interaction between the branches due to the high density of the branches. Considering the same temperature dependence of two shift factors, $a_{T,M}$ and $a_{T,B}$, we concluded that the main chain component and the branch component have the very similar activation energy for orientation relaxation of each component.

AUTHOR INFORMATION

Corresponding Author

*E-mail: tadashi@chem.sci.osaka-u.ac.jp.

ACKNOWLEDGMENT

One of the authors (H. Iwawaki) expresses his special thanks for the Global COE (center of excellence) Program "Global Education and Research Center for Bio-Environmental Chemistry" of Osaka University. This work was partly supported by Grant-in-Aid for Scientific Research on Priority Area "Soft

Matter Physics" from the Ministry of Education, Culture, Sports, Science and Technology, Japan (Nos. 18068009 and 20340112).

REFERENCES

(1) Doi, M.; Edwards, S. F. *The Theory of Polymer Dynamics*; Clarendon: Oxford, U.K., 1986.
(2) Larson, R. G. *Macromolecules* **2004**, *37*, 5110–5114.
(3) Inoue, T. *Macromolecules* **2006**, *39*, 4615–4618.
(4) Inoue, T.; Okamoto, H.; Osaki, K. *Macromolecules* **1991**, *24*, 5670–5675.
(5) Inoue, T.; Osaki, K. *Macromolecules* **1996**, *29*, 1595–1599.
(6) Rathgeber, S.; Pakula, T.; Wilk, A.; Matyjaszewski, K.; Beers, K. L. *J. Chem. Phys.* **2005**, *122*, 124904.
(7) Wintermantel, M.; Gerle, M.; Fischer, K.; Schmidt, M.; Wataoka, I.; Urakawa, H.; Kajiwara, K.; Tsukahara, Y. *Macromolecules* **1996**, *29*, 978–983.
(8) Nemoto, N.; Nagai, M.; Koike, A.; Okada, S. *Macromolecules* **1995**, *28*, 3854–3859.
(9) Wintermantel, M.; Schmidt, M.; Tsukahara, Y.; Kajiwara, K.; Kohjiya, S. *Macromol. Rapid Commun.* **1994**, *15*, 279–284.
(10) Terao, K.; Takeo, Y.; Tazaki, M.; Nakamura, Y.; Norisuye, T. *Polym. J.* **1999**, *31*, 193–198.
(11) Terao, K.; Nakamura, Y.; Norisuye, T. *Macromolecules* **1999**, *32*, 711–716.
(12) Terao, K.; Hokajo, T.; Nakamura, Y.; Norisuye, T. *Macromolecules* **1999**, *32*, 3690–3694.
(13) Hokajo, T.; Terao, K.; Nakamura, Y.; Norisuye, T. *Polym. J.* **2001**, *33*, 481–485.
(14) Nakamura, Y.; Norisuye, T. *Polym. J.* **2001**, *33*, 874–878.
(15) Namba, S.; Tsukahara, Y.; Kaeriyama, K.; Okamoto, K.; Takahashi, M. *Polymer* **2000**, *41*, 5165–5171.
(16) Tsukahara, Y.; Namba, S.; Iwasa, J.; Nakano, Y.; Kaeriyama, K.; Takahashi, M. *Macromolecules* **2001**, *34*, 2624–2629.
(17) Janeschitz-Kriegl, H. *Polymer Melt Rheology and Flow Birefringence*; Springer-Verlag: Berlin, 1983.
(18) Volkenstein, M. V.,*Configurational Statistics of Polymeric Chains*; Interscience: New York, 1963.
(19) Flory, P. J. *Statistical Mechanics of Chain Molecules*; John Wiley & Sons: New York, 1969.
(20) Inoue, T.; Matsuno, K.; Watanabe, H.; Nakamura, Y. *Macromolecules* **2006**, *39*, 7601–7606.
(21) Kalogrianitis, S. G.; vanEgmond, J. W. *J. Rheol.* **1997**, *41*, 343–364.
(22) Tsukahara, Y.; Inoue, J.; Ohta, Y.; Kohjiya, S.; Okamoto, Y. *Polym. J.* **1994**, *26*, 1013–1018.
(23) Nakamura, Y.; Koori, M.; Li, Y.; Norisuye, T. *Polymer* **2008**, *49*, 4877–4881.
(24) Hayashi, C.; Inoue, T. *Nihon Reoroji Gakkaishi* **2009**, *37*, 205–210.
(25) Hutcheson, S. A.; McKenna, G. B. *J. Chem. Phys.* **2008**, *129*, 074502 .
(26) Schroter, K.; Hutcheson, S. A.; Shi, X.; Mandanici, A.; McKenna, G. B. *J. Chem. Phys.* **2006**, *125*, 214507.
(27) Onogi, T.; Inoue, T.; Osaki, K. *Nihon Reoroji Gakkaishi* **1998**, *26*, 237–241.
(28) Ferry, J. D.,*Dependence of Viscoelastic Behavior on Temperature and Pressure*, 4th ed.; Wiley: New York, 1980; pp 264−320.
(29) Vlassopoulos, D.; Fytas, G.; Loppinet, B.; Isel, F.; Lutz, P.; Benoit, H. *Macromolecules* **2000**, *33*, 5960–5969.
(30) Pakula, T.; Zhang, Y.; Matyjaszewski, K.; Lee, H. I.; Boerner, H.; Qin, S. H.; Berry, G. C. *Polymer* **2006**, *47*, 7198–7206.
(31) Roovers, J.; Graessley, W. W. *Macromolecules* **1981**, *14*, 766–773.
(32) Kirkwood, K. M.; Leal, L. G.; Vlassopoulos, D.; Driva, P.; Hadjichristidis, N. *Macromolecules* **2009**, *42*, 9592–9608.
(33) Ham, J. S. *J. Chem. Phys.* **1957**, *26*, 625–633.
(34) Rouse, P. E. *J. Chem. Phys.* **1953**, *21*, 1272–1280.
(35) Yamamoto, S.; Ejaz, M.; Tsujii, Y.; Fukuda, T. *Macromolecules* **2000**, *33*, 5608–5612.